

Methane Formation in H₂,CO Mixtures over Carbon-Supported Potassium Carbonate

R. MEIJER, R. VAN DOORN, F. KAPTEIJN,¹ AND J. A. MOULIJN²

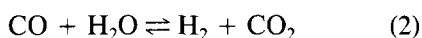
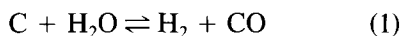
Department of Chemical Engineering, University of Amsterdam, Nieuwe Achtergracht 166, 1018 WV Amsterdam, The Netherlands

Received October 17, 1990; revised July 5, 1991

The rates of CH₄ and CO₂ formation over K₂CO₃/carbon have been studied in H₂,CO mixtures as a function of temperature (600–1000 K), total pressure (1.5–10 bar), H₂/CO feed ratio (0.3–8), and the K₂CO₃ loading (0–20 wt%). In H₂,CO mixtures both the rate of CH₄ and CO₂ formation are enhanced by the presence of the potassium catalyst and show the same dependence on the alkali loading as that observed for gasification of carbon in H₂O and CO₂. Below 900 K the CH₄ formation has an apparent order of ≈ 1.2 in p_{H_2} and ≈ 0.3 in p_{CO} . Under most experimental conditions the rate of CO₂ formation ($E_a(\text{app}) = 40\text{--}50 \text{ kJ mol}^{-1}$) is higher than that of CH₄ formation ($E_a(\text{app}) = 130\text{--}150 \text{ kJ mol}^{-1}$), resulting in carbon deposition. Only at pressures above 5 bar can CO be selectively converted with H₂ into CH₄ and CO₂ above 900 K. Hydrogenation of the support and of the carbon deposited by the CO disproportionation is not catalysed by potassium. A reactive carbon intermediate is proposed, formed by catalysed dissociation of CO. This can either react with hydrogen to form methane or form the carbon deposit. The oxygen is removed by CO in a manner similar to that in potassium-catalysed oxygen exchange reactions. The observed deactivation is ascribed to a combined effect of blocking of the active sites by carbon deposition and migration of metallic potassium into the carbon matrix, leading to H₂ adsorption on the liberated carbon edge sites, as revealed by temperature-programmed desorption. Potassium is hardly lost at all during the methanation experiments. © 1992 Academic Press, Inc.

INTRODUCTION

The methanation reaction (Eq. (3)) is one of the principal reactions taking place during steam gasification of carbonaceous materials, a process that can be described by a set of three independent reactions:



Extensive research has been conducted on the kinetics and mechanism of the alkali-catalysed steam gasification, but this was predominantly performed under conditions

at which methane formation could be neglected (low pressure, relatively high temperature). It is known that the rate of alkali-catalysed gasification of carbon by steam (1) and the water gas shift (WGS) (2) reaction sharply increase with increasing temperature, whereas the production of methane by Eq. (3) at higher temperatures is limited by thermodynamic equilibrium (3). Operating the gasification process at temperatures below 1000 K and at elevated pressures increases the overall methane yield (4). In contrast to the gasification (Eq. (1)) and WGS reaction (Eq. (2)), only a limited number of studies (4–11) have reported on the alkali-catalysed methanation reaction. It appears that the catalytic action of alkali metals in the formation of methane is poorly understood. Research on the formation of methane during potassium-catalysed coal gasification at elevated pressure and low

¹ To whom correspondence should be addressed.

² Present address: Department of Chemical Engineering and Materials Science, Delft University of Technology, Julianalaan 136, Delft, The Netherlands.

temperature ($P = 35$ bar, $T = 700^\circ\text{C}$) was performed by Exxon (4). In the Exxon catalytic coal gasification (CCG) process the liberated heat of formation of methane was used for the endothermic gasification of coal producing CO and H_2 (autothermal gasification), thus obtaining an overall thermoneutral process. Alkali-catalysed methane formation might well be interesting for applications outside coal gasification. An advantage of alkali catalysts over, e.g., group VIII metal catalysts (12, 13), is their tolerance to traces of H_2S present (9).

The aim of this study was to examine the role of potassium in the methane formation. This was performed by studying the rate of methane formation from H_2 , CO reactant mixtures over carbon-supported potassium carbonate, as a function of temperature, total pressure, K_2CO_3 loading, and H_2/CO feed ratio.

EXPERIMENTAL

Apparatus

The fixed-bed flow system used in this study is described in detail elsewhere (14, 15). Basically it consists of a gas mixing section, an oven ($T_{\text{max}} = 1273$ K) containing the catalyst/carbon sample in a quartz tube (i.d. = 3–7 mm), and a gas chromatograph for product analysis (dual column, He carrier, TCD). The experiments are performed in a ceramic (2–10 bar) or quartz (1.5 bar) reactor.

Sample Preparation

The model carbon used in this study is Norit RX1 extra, an acid-washed, steam-activated peat char with a high surface area ($1100\text{ m}^2\text{ g}^{-1}$ (CO_2 adsorption at 273 K), $1500\text{ m}^2\text{ g}^{-1}$ (N_2 adsorption at 77 K), particle size 0.25–0.6 mm, 3 wt% ash). K_2CO_3 (0–20 wt%) was added by pore volume impregnation with an aqueous solution of this salt. The initial loading is expressed as the atomic potassium to carbon (K/C)_i ratio. The amount of potassium still present in the catalyst/carbon samples after different treatment is removed by acid washing (2%

HNO_3) and measured by ICP–AES, which in an earlier study (16) has proven to be a good quantitative technique.

Experimental Procedures

For each methanation experiment, a reproducible sample was obtained by drying *in situ* ($T = 473$ K, He) followed by isothermal gasification ($T = 1000$ K, $P_t = 1.5$ bar, $F_t = 140\ \mu\text{mol s}^{-1}$, $p_{\text{H}_2\text{O}} = 0.5$ bar, balance He) to a steady-state gasification level (20 to 30% burnoff) (16). Subsequently, the sample is cooled to 600 K and the H_2 , CO, He gas mixture is passed over the sample. The rate of methane formation is measured during a temperature-programmed reaction (TPR) cycle (600–1000–600 K), in which a temperature gradient (β) of 5 K min^{-1} and an isothermal period of 35 min at 1000 K is applied. The rates of CH_4 and CO_2 formation, $r(\text{CH}_4)$ and $r(\text{CO}_2)$, respectively, are expressed as mol CH_4 or CO_2 produced (mol potassium initially present)⁻¹ s⁻¹. Carbon deposition is expressed as the cumulated amount of carbon deposited in $\mu\text{mol C}$.

The rate of CH_4 and CO_2 formation and the net amount of carbon deposition have been studied as a function of temperature ($T = 600$ –1000 K), total pressure ($P_t = 1.5$ –10 bar), catalyst loading (0–20 wt% K_2CO_3), and H_2/CO feed ratio ($R = 0.3$ –8.0) with a total flow of $140\ \mu\text{mol s}^{-1}$ (balance He) and initial sample size of 300 mg (Table 1). Some additional TPR experiments that were carried out are explained in the text.

Temperature-programmed desorption (TPD) patterns were obtained in a helium flow of $20\ \mu\text{mol s}^{-1}$ at a heating rate (β) of 10 K min^{-1} , followed by an isothermal period of 30 min at 1200 K.

Data Handling

During TPR in H_2 , CO mixtures, besides CH_4 formation a much larger amount of CO_2 production is observed. This “excess” CO_2 can originate either from CO disproportionation (Eq. (4)) or the WGS reaction (Eq. (2)). Because no H_2O production was observed and CO_2 production was also ob-

TABLE 1

Experimental Conditions Applied in This Study

Variable	P_t (bar)	$(K/C)_i$	$R = (p_{H_2}/p_{CO})$ feed
p_{CO}^a (bar)	0		∞
	0.0625		8
	0.1	1.5	5
	0.5		1
	1.0		0.5
$p_{H_2}^b$ (bar)	0		0
	0.15	1.5	0.3
	0.5		1
	1.0		2
P_t (bar)	1.5		
	5.0	0.019	2
	10		
$(K/C)_i$ (mol/mol)		0.0	
		0.009	
	1.5	0.019	2
		0.031	
		0.043	

^a $p_{H_2} = 0.5$ bar.

^b $p_{CO} = 0.5$ bar.

served in the absence of H_2 (Fig. 4, $p_{H_2} = 0$), obviously CO disproportionation (Eq. (4)) takes place under the applied conditions (7, 9). Furthermore, from the absence of H_2O in the product gas it was concluded that no WGS takes place. Furthermore, CH_4 formation by $CO + H_2 \rightarrow CH_4 + H_2O$ can be excluded



From the GC analysis data and an overall mass balance, taking into account the changing molar flow rate (Eqs. (3) and (4)), the rates of CH_4 and CO_2 formation were calculated. The difference $r(CO_2) - r(CH_4)$ then equals the rate of carbon deposition and, hence, the total amount of carbon deposition could be calculated. Under all experimental conditions the reactor can be described as a differential reactor (CO conversion <2%). Also the CH_4 formation rate is sufficiently low not to be affected by thermodynamic equilibrium, so only the forward reaction rate of Eq. (3) is studied.

RESULTS

In Fig. 1, characteristic CH_4 and CO_2 formation patterns obtained during a temperature-programmed reactivity measurement are shown. The arrows indicate the heating

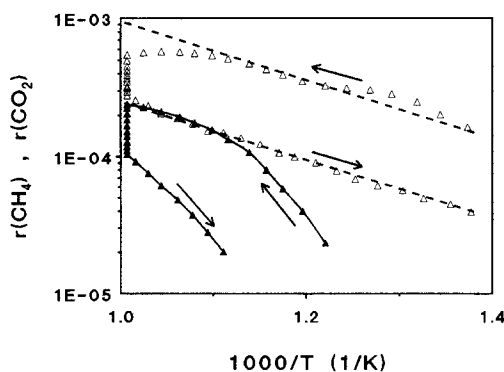


FIG. 1. A characteristic pattern for $r(CH_4)$ (▲) and $r(CO_2)$ (Δ) during TPR as a function of the reciprocal temperature ($K/C_i = 0.019$, $R = 2$, $P_t = 1.5$ bar). The arrows indicate the heating and cooling stage in the TPR experiment.

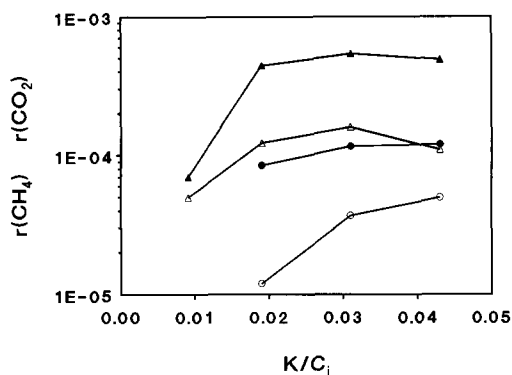


FIG. 2. $r(\text{CH}_4)$ (●○) and $r(\text{CO}_2)$ (▲△) at 870 K during the heating (solid symbols) and cooling (open symbols) stage of the TPR experiment as a function of the (K/C_i) ratio ($R = 2$, $P_t = 1.5$ bar).

and cooling stage of the experiment. This figure illustrates the general observation that $r(\text{CO}_2)$ is much larger than $r(\text{CH}_4)$, indicating that under these conditions carbon is deposited on the catalyst/carbon sample. During the heating stage, the changing slope in Fig. 1 suggests an apparent deactivation of the catalyst for CO_2 and CH_4 formation, which progresses during the isothermal period at 993 K. The low rates observed for CH_4 formation over these K_2CO_3 /carbon samples exclude the possibility that mass transport limitations are responsible for the changing slope (2, 14, 18).

In the cooling stage of the TPR experiment the rate of CH_4 formation is lower than that in the heating state but the slopes of both curves ($-E_a/R$) are the same at similar temperatures. The rate of CO_2 formation is higher than of CH_4 indicating that under these conditions carbon is deposited, and, although less pronounced, shows a similar behaviour as observed for $r(\text{CH}_4)$.

In Fig. 2 $r(\text{CH}_4)$ and $r(\text{CO}_2)$ are shown at 870 K in both the heating and cooling stage of the TPR experimental for samples with different K/C_i ratio. As can be seen, both the CH_4 and CO_2 formation are influenced by the amount of K_2CO_3 present, whilst pure carbon (not shown) showed a negligible CO_2 and no detectable CH_4 formation under

these conditions. The difference in CH_4 formation rate at 870 K between the heating and cooling stage of the experiment, $\Delta r(\text{CH}_4)$, becomes smaller for samples with increasing K/C_i ratio (Table 2). Such a trend is not observed for $r(\text{CO}_2)$.

In Fig. 3 the influence of the partial CO pressure ($p_{\text{H}_2} = 0.5$ bar) on the rates of CH_4 and CO_2 formation at 870 K, in the heating and cooling stage of the TPR experiment over a $K/C_i = 0.019$ sample, is shown. Generally, with increasing p_{CO} an increase in both $r(\text{CH}_4)$ and $r(\text{CO}_2)$ is observed, which level off or decrease slightly at high p_{CO} . The apparent orders in CO are about 0.8 and 0.3 for CO_2 and CH_4 formation, respectively.

In Fig. 4 the influence of the partial H_2 pressure ($p_{\text{CO}} = 0.5$ bar) on the rates of CH_4 and CO_2 formation over a $K/C_i = 0.019$ sample at 870 K is shown. The rate of CH_4 formation shows a positive order of about 1.2 in p_{H_2} (p_{CO} constant), whereas the rate of CO_2 formation, even in the absence of H_2 , remains fairly constant.

From the experimental data it can be calculated that in the temperature region, where no apparent deactivation is observed ($T \leq 870$ K) the apparent activation energies for CH_4 and CO_2 formation are 130–150 and 40–50 kJ mol^{-1} , respectively.

Figure 5 shows the influence of total pressure at constant H_2/CO ratio ($R = 2$) on the rates of CH_4 and CO_2 formation over a 10 wt% K_2CO_3 /carbon sample during TPR. Both rates increase with increasing total pressure. At low total pressure $r(\text{CH}_4)$ is smaller than $r(\text{CO}_2)$. With increasing pressure $r(\text{CH}_4)$ increases much faster than $r(\text{CO}_2)$ and at $P_t = 5$ and 10 bar and above 850 K, $r(\text{CH}_4)$ becomes equal or slightly exceeds $r(\text{CO}_2)$. The degree of deactivation during the isothermal period at 993 K and the net amount of carbon deposition are less at higher total pressure.

The effect of two consecutive TPR cycles on the rate of CH_4 formation over a 20 wt% K_2CO_3 /carbon sample ($R = 2$, $P_t = 1.5$ bar) is given in Fig. 6. The rate of methane formation during the cooling stage of the first and

TABLE 2

The Total Amount of Carbon Deposited and Potassium Lost, Together with $r(\text{CH}_4)$ at 870 K in the Heating Stage and Its Percentage Decrease between the Heating and the Cooling Stage of the Experiment, $\Delta r(\text{CH}_4)$, as a Function of the H_2/CO Feed Ratio (R), Total Pressure (P_t), and Initial K_2CO_3 Loading

	C deposited (μmol)	$r(\text{CH}_4)_{\text{heating}}$ 870 K ($\mu\text{mol mol K}_i^{-1}$ s^{-1})	K loss (%)	$\Delta r(\text{CH}_4)(\%)$ $T = 870 \text{ K}$
$R = p_{\text{H}_2}/p_{\text{CO}} (P_t = 1.5 \text{ bar}; K/C_i = 0.019)$				
0	1864	—	—	—
0.3	1385	—	38	—
0.5	1559	68	57 ^a	100
1	1394	58	34	100
2	797	85	41	88
5	174	39	31	62
8	178	30	33	60
∞	—	—	—	—
P_t (bar) ($R = 2; K/C_i = 0.019$)				
1.5	797	85	41	88
5	642	450	40	77
10	-400	751	40	40
wt% K_2CO_3 ($R = 2; P_t = 1.5 \text{ bar}$)				
5	243	—	60	—
10	797	85	41	88
15	1263	116	42	68
20	876	120	35	58

^a After TPR gasified in H_2O , He at 1000 K up to 80% burnoff.

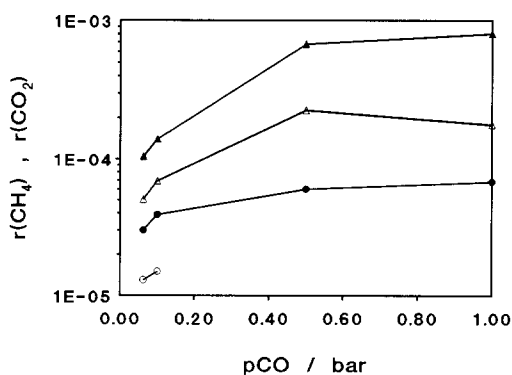


FIG. 3. $r(\text{CH}_4)$ (○●) and $r(\text{CO}_2)$ (△▲) at 870 K during the heating (solid symbols) and cooling (open symbols) stage of the TPR experiment. Variation of p_{CO} (bar) at constant p_{H_2} . $K/C_i = 0.019$; $p_{\text{H}_2} = 0.5 \text{ bar}$, $P_t = 1.5 \text{ bar}$.

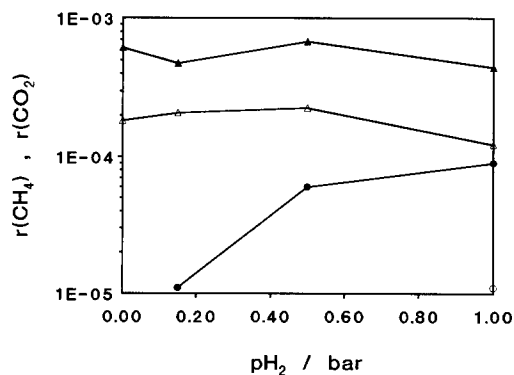


FIG. 4. $r(\text{CH}_4)$ (○●) and $r(\text{CO}_2)$ (△▲) at 870 K during the heating (solid symbols) and cooling (open symbols) stage of the TPR experiment. Variation of p_{H_2} (bar) at constant p_{CO} . $K/C_i = 0.019$; $p_{\text{CO}} = 0.5 \text{ bar}$, $P_t = 1.5 \text{ bar}$.

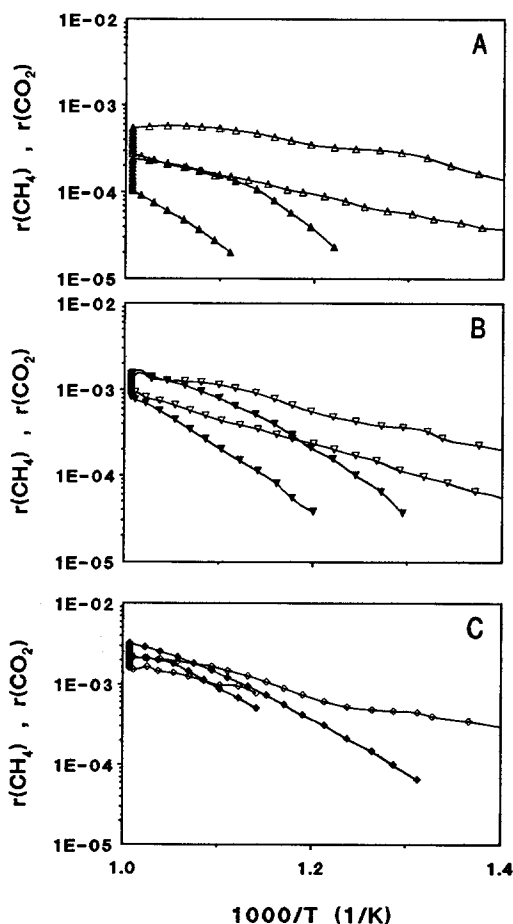


FIG. 5. $r(\text{CH}_4)$ (solid symbols) and $r(\text{CO}_2)$ (open symbols) at different total pressure during TPR (H_2/CO $R = 2$) with a $K/C_i = 0.019$ sample. $P_t = 1.5$ bar (A); $P_t = 5$ bar (B); and $P_t = 10$ bar (C).

the heating stage of the second cycle are equal to approximately 900 K, whereas above this temperature an irreversible deactivation is observed.

In order to compare the activity of the carbon support and that of the deposited carbon towards hydrogenation, the rate of methane formation during a TPR in H_2/He (15% H_2) was measured for a sample after the gasification pretreatment (Fig. 7A) and a sample that additionally had undergone a TPR in CO/He (33% CO ; Fig. 7B). The pretreatment of the sample in CO resulted in approximately 9% weight gain, calculated

from the 1864 μmol CO_2 produced (Eq. (4)). In both TPR(H_2) experiments, not only CH_4 production but also CO_2 and CO are observed. The CO evolution parallels that of CH_4 , but is one order of magnitude larger (Table 3).

The TPD pattern obtained directly after SSG($\text{H}_2\text{O}/\text{He}$) and TPR(H_2/CO $R = 2$) (Fig. 8A) shows remarkable differences compared with a TPD pattern obtained directly after partial gasification in H_2O (Fig. 8B) or in CO_2 (16, 17). After H_2O or CO_2 gasification, CO is observed as the main desorption product between 1000 and 1100 K and H_2 is only observed above 1150 K after gasification in H_2O or $\text{H}_2\text{O}/\text{H}_2$ mixtures (Fig. 8B). During TPD after TPR in a H_2/CO ($R = 2$) mixture a completely different desorption pattern is obtained. Between 600 and 1000 K, simultaneously H_2 , CO and CO_2 are observed, above 1000 K H_2 has become the main desorption product, whereas the CO evolution between 1000 and 1200 K is considerably smaller. The amounts of desorption products relative to the amount of potassium actually present in the sample are given in Table 4.

DISCUSSION

The rate of methane formation per mol of potassium initially present (Fig. 2) shows a

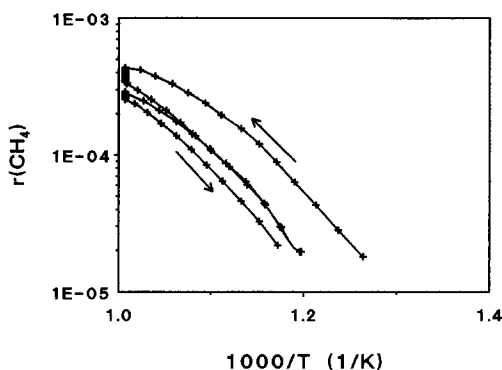


FIG. 6. $r(\text{CH}_4)$ during two consecutive TPR(H_2/CO $R = 2$) cycles over a 20 wt% K_2CO_3 /carbon sample ($P_t = 1.5$ bar). The numbered arrows refer to the heating stage in the first and the cooling stage in the second cycle.

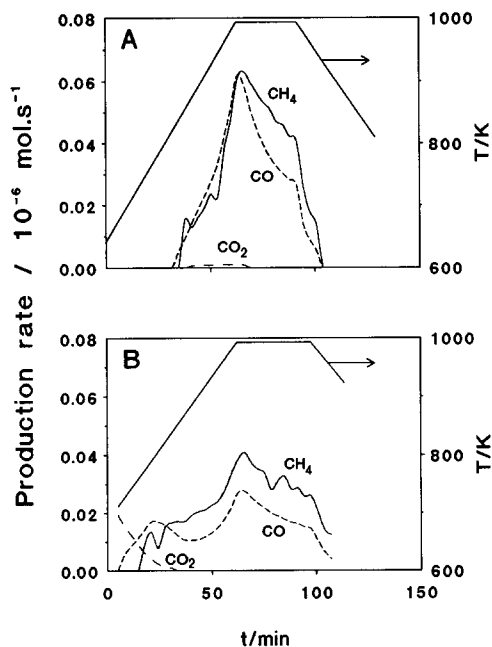


FIG. 7. TRP(15% H₂) of a 10 wt% K₂CO₃/carbon sample. Pretreatment: (A) SSG(H₂O, He $T = 1000$ K). (B) SSG(H₂O, He $T = 1000$ K) followed by TPR (33% CO) (the CH₄ production rate in both plots has been multiplied by a factor of 10).

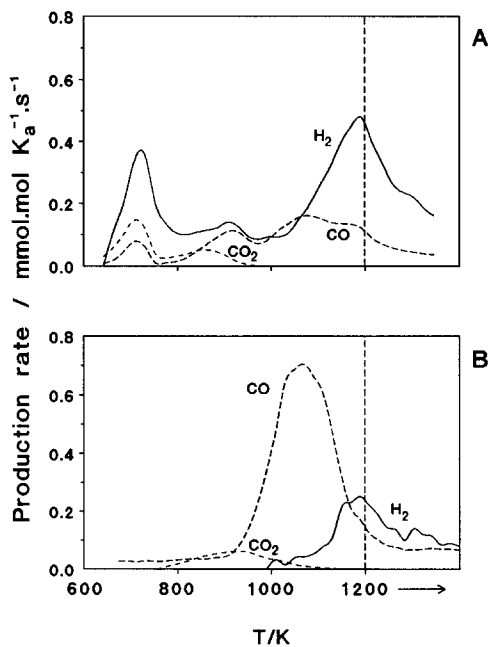


FIG. 8. TPD patterns in helium up to 1200 K for $K/C_i = 0.019$ samples after different treatments: (A) SSG(H₂O, He) followed by TPR(H₂, CO, $R = 2$). (B) SSG(H₂O, He).

similar dependence on the initial K/C ratio as the rate of gasification in CO₂ (14, 16, 18) and H₂O (2) and of water gas shift (2) reactions (Fig. 9). The methanation activity per mol potassium initially present, $r(\text{CH}_4)$, taken from the heating stage of the TPR experiment, shows a slight increase with increasing potassium to carbon ratio between 0.019 and 0.043, similar to that observed for

the gasification activity. Obviously, potassium catalyses the CH₄ production. Furthermore, it is striking that the samples with low initial catalyst loading suffer a stronger deactivation with respect to the CH₄ formation as compared to the samples with a higher initial catalyst loading.

From Figs. 1 to 4 and Fig. 6 it can be seen that the total amount of CO₂ formed during a TPR(H₂, CO) experiment is generally much

TABLE 3

Total Amount of Products (μmol) Observed in Different TPR Experiments over a K₂CO₃/Carbon Sample after SSG(H₂O, He) up to $\pm 25\%$ Burnoff ($K/C = 0.019$; $K_{\text{initial}} = 400 \mu\text{mol}$)

Treatment	CO	CO ₂	CH ₄
TPR(H ₂)	125	2	15
TPR(H ₂) after TPR(CO)	95	14	15
TPR(CO)	—	1864	—

TABLE 4

Total Amounts of Desorption Products Relative to the Amount of Potassium Actually Present^a (mol/mol), Observed in TPD after Different Treatment ($K/C_i = 0.019$; $P_1 = 1.5$ bar)

Treatment	H ₂ /K _a	CO/K _a	CO ₂ /K _a
SSG(H ₂ O, He) and TPR(H ₂ , CO)	0.84	0.33	0.10
SSG(H ₂ O, He)	0.34	0.86	0.07
SSG(CO ₂) (from (16))	—	0.90	0.22

^a Data corrected for the amount of potassium lost (16).

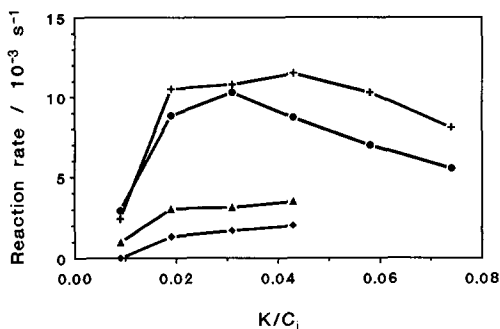


FIG. 9. Steady-state reaction rates ($\text{mol} \cdot \text{K}_i^{-1} \cdot \text{s}^{-1}$) as a function of the initial K/C ratio of the catalyst/carbon sample for CO_2 (▲) and H_2O (+) gasification at 1000 K, $\text{H}_2\text{O}/\text{CO}$ (●) oxygen exchange at 833 K and CH_4 (◆) formation at 870 K (multiplied by a factor of 10).

larger than the amount of CH_4 produced, indicating that under these conditions CO disproportionation is the predominant reaction (7, 9). Due to the stronger H_2 pressure dependence and higher activation energy the rate of CH_4 formation increases more than the CO_2 production with increasing temperature and pressure. Above 5 bar and 900 K CO can be selectively hydrogenated to CH_4 . At lower temperatures and pressures the selectivity for CH_4 is lower and carbon is deposited. The total weight gain increases up to 9 wt% (TPR in CO). This is of the same order of magnitude as observed by Walker *et al.* (7) for a potassium-loaded lignite char. The deposited carbon does not seem to be hydrogenated to CH_4 , which is confirmed by TPR(H_2) experiments. These TPR(H_2) experiments show that a preceding TPR in CO does not result in an increased amount of CH_4 produced (Fig. 7, Table 3).

In both TPR(H_2) experiments (with or without a preceding TPR(CO)) only a small amount of CH_4 is formed ($\sim 15 \mu\text{mol}$), while its production pattern parallels the more extensive CO desorption pattern. This suggests that the methane formation in these experiments is a secondary reaction of desorbed CO with H_2 (Eq. (3)) and there is no direct hydrogenation of deposited carbon or of the support.

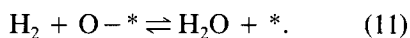
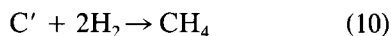
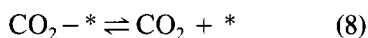
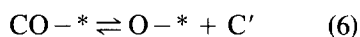
The above mentioned results indicate that the potassium catalyst enhances the formation of CH_4 from H_2 , CO and of CO_2 from CO, and hence the C deposition, but potassium does not catalyse the hydrogenation of the deposited carbon under the applied conditions.

This result suggests that during TPR in H_2 , CO a reactive carbon (C') is formed on the active site. Consecutively, this reactive carbon can either be hydrogenated to CH_4 or form a carbon deposit ($\text{C} \downarrow$) on the sample; the selectivity for CH_4 is favoured by higher pressures and temperatures. The observed activation energy for the CH_4 formation ($130\text{--}150 \text{ kJ mol}^{-1}$) is lower than generally found for the hydrogen gasification of carbonaceous materials ($150\text{--}200 \text{ kJ mol}^{-1}$) (3) and reflects the reactive nature of the intermediate.

The carbon deposit has become inactive for hydrogenation under the conditions investigated. Walker *et al.* (7) observed that carbon deposited by CO disproportionation at 1123 K is highly reactive during potassium-catalysed gasification in H_2O , which indicates that an oxidising species, i.e., H_2O or O_2 and/or a higher temperature (cf. Fig. 5C) is needed to gasify this deposited carbon.

From a recent thermogravimetric study (19) it was concluded that, in the presence of CO_2 or H_2O , H_2 hardly interacts with the catalyst/carbon sample at 650 K, whereas both CO and CO_2 show a strong interaction with the reduced alkali catalyst (*) leading to formation of $\text{O}-*$ and CO_2-* (Eqs. (5)–(8)), which are intermediates in alkali-catalysed gasification and oxygen exchange reactions (2, 16, 18–20). In this notation the asterisk (*) represents the reduced active site, which is envisaged as a partially reduced alkali oxide cluster. Due to the gasification pretreatment, at the start of the methanation experiments the active sites will mainly be in the oxidised ($\text{O}-*$) or chemisorbed (CO_2-*) state (19, 20). Meijer *et al.* (19) have shown that these sites can be reduced by H_2 through Eq. (11) or can inter-

act with CO to form $\text{CO}_2 - *$ (Eq. (7)). Because during TPR in H_2, CO no H_2O was produced the latter is most likely to occur. This corresponds with the observations of Meijer *et al.* (2, 19) that in the presence of gas phase CO and H_2 the oxidised site ($\text{O} - *$) predominantly interacts with CO to form $\text{CO}_2 - *$. From the presented and earlier reported results the interaction of CO with the reduced active site ($*$) leading to carbon deposition and CO_2 formation can be represented by Eqs. (5) to (9). In this scheme C' represents the reactive carbon, which can either react with hydrogen to form CH_4 (Eq. (10)), or forms the carbon deposit $\text{C} \downarrow$ (Eq. (9)), which is inactive for hydrogenation under the applied conditions.



The active site in alkali-catalysed gasification ($*$) is generally described as a small cluster of the alkali oxide, here K_xO_y ($x \geq y$), anchored via phenolate groups at the edges of the graphitic planes of the carbon substrate (16, 18–20). The cluster size depends on the catalyst loading (16). During TPD the cluster is reduced and the phenolate, is decomposed, resulting in CO desorption at 1000–1100 K (Fig. 8B). Above 1100 K C–H bonds that terminate the carbon edges dissociate and H_2 is released. After exposure of the potassium oxide/carbon sample to the methanation conditions the oxygen content of the cluster has been reduced by a factor of three, since less CO is released (Table 4). Also a number of phenolate groups must have been decomposed and hydrogen atoms now terminate the carbon edge atoms. This is reflected by the

increased hydrogen desorption above 1050 K (21, 22).

The desorption of CO_2 , CO, and H_2 around 700 K is ascribed to adsorption at the active sites. At these temperatures it has been shown by application of $^{13}\text{CO}_2$ (25) that CO_2 does not react with a reduced catalyst/carbon system. Only above 800 K does the desorbing CO_2 oxidise the catalyst, resulting in the CO formation at 900 K. In summary, TPD indicates that the active catalyst under methanation conditions can be best indicated by a reduced potassium oxide species of an average stoichiometry of $\text{KO}_{0.3}$.

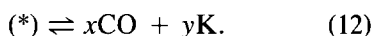
Deactivation

Figure 6 shows that during two successive TPR(H_2, CO $R = 2$) cycles the rate of CH_4 formation is equal during the cooling stage of the first and the heating stage of the second cycle up to approximately 900 K, but that during the second cooling stage a lower methane production is observed. This suggests that at low total pressure and in a reducing (H_2, CO) atmosphere deactivation only takes place at high temperatures and is irreversible upon cooling.

In other studies (7, 9–11) deactivation of the alkali catalyst for CH_4 formation is ascribed to either carbon deposition on the active sites or loss of active catalyst by evaporation of the reduced alkali catalyst. However, the 30 to 40% potassium loss observed in these experiments (Table 2) can be ascribed to catalyst loss during the initial stages of burnoff in the gasification pretreatment of the catalyst/carbon sample (16, 24). This rules out the second possibility. Only in two cases in which a low initial loading was used and the sample was gasified up to 80% burnoff after TPR in H_2, CO was a higher loss of potassium observed. The first can be attributed to the low K_2CO_3 loading ($K/C = 0.0091$), which has proven to be ineffective for gasification (17) whereas in the second case the high burnoff provides a plausible explanation for the high amount of potassium loss.

Table 2 shows that the percentage de-

crease in CH_4 formation at 870 K increases with decreasing $p_{\text{H}_2}/p_{\text{CO}}$ ratio in the feed, which is accompanied by an increasing amount of carbon deposition during the TPR experiment. Therefore, carbon deposition, blocking active sites, seems to be an important factor. However, under conditions at which no net carbon deposition is observed ($P_1 = 5$ and 10 bar, $T > 850$ K, Figs. 5B and 5C), a considerable deactivation in the CH_4 and CO_2 formation is also observed, indicating that blocking sites by carbon is not the only explanation. At these temperatures and in a reducing gas phase the active sites can be reduced to the metallic state (Eq. (12)) and it has been observed that potassium subsequently migrates into the carbon matrix, becoming unavailable for catalytic action (16, 23).



This combined effect of carbon deposition and migration of active catalyst into the carbon matrix provides a plausible explanation for the observed deactivation above 900 K in the TPR experiments. Under the gas phase conditions applied, migration of metallic potassium is irreversible, whereas blocking of active catalyst by carbon deposition can be prevented by operation at elevated pressures and above 850 K, conditions at which no net carbon deposition takes place.

CONCLUSIONS

The rates of CH_4 and CO_2 formation, applying H_2 , CO mixtures, are enhanced by the addition of K_2CO_3 to an activated carbon support. For the CH_4 formation below 900 K an apparent order in p_{H_2} of about 1.2 and in p_{CO} of ≈ 0.3 is observed. At low total pressure, or low $p_{\text{H}_2}/p_{\text{CO}}$ ratio the selectivity for CH_4 is low and mainly the formation of CO_2 and inactive carbon, deactivating the catalyst, is observed. The stronger p_{H_2} and temperature dependence of the CH_4 formation results in a selective conversion of CO to CH_4 and CO_2 at high total pressures and sufficient $p_{\text{H}_2}/p_{\text{CO}}$ ratio above 900 K. This explains the possibility of direct methane

formation over potassium/carbon systems in gasification.

It is envisaged that from CO a reactive carbon intermediate is formed on the catalyst. This can either be hydrogenated to CH_4 or can form a carbon deposit on the sample. The oxygen is removed by CO with formation of CO_2 . Hydrogenation of the carbon deposit and of the support is not catalysed by potassium. The observed overall deactivation is due to a combined effect of blocking the active sites by carbon deposition and migration of metallic potassium into the carbon matrix.

The active site is best indicated by a highly reduced potassium oxide under the methanation conditions. Due to the partial reduction of the potassium oxide carbon edge atoms are liberated, which subsequently adsorb hydrogen. This results during TPD in an increased hydrogen desorption, compared to samples treated in H_2O or CO_2 . Potassium is only lost during the gasification pretreatment and not under the methanation conditions.

ACKNOWLEDGMENT

These investigations have been executed within the framework of the Dutch National Coal Research Programme (NOK), which is managed by the Project Office for Energy Research (NOVEM) and financed by the Ministry of Economic Affairs.

REFERENCES

1. Kapteijn, F., Niamut, H. F. A., and Moulijn, J. A., in "Proceedings, Carbon '86, Baden-Baden, FRG," p. 537, 1986.
2. Meijer, R., Sibeijn, M., van Dillen, M. R. B., Kapteijn, F., and Moulijn, J. A., *I & E C Res.*, **30**, 1760 (1991).
3. Kapteijn, F., and Moulijn, J. A., in "Carbon and Coal Gasification: Science and Technology" (J. L. Figueiredo and J. A. Moulijn, Eds.), p. 291. Nijhoff, The Hague, 1986.
4. Nahas, N. C., *Fuel* **62**, 239 (1983).
5. Cabrera, A. L., Heinemann, H., and Somorjai, G. A., *Chem. Phys. Lett.* **81**, 402 (1981).
6. Cabrera, A. L., Heinemann, H., and Somorjai, G. A., *J. Catal.* **75**, 7 (1982).
7. Walker, P. L., Jr., Matsomoto, S., Hanzawa, T., Miura, T., and Ismail, I. M. K., *Fuel* **62**, 140 (1983).
8. Casanova, R., Cabrera, A. L., Heinemann, H., and Somorjai, G. A., *Fuel* **62**, 1138 (1983).

9. Kapteijn, F., and Moulijn, J. A., *J. Chem. Soc. Chem. Commun.*, 278 (1984).
10. Otake, T., Tone, S., Kimura, S., and Hino, Y., *J. Chem. Eng. Jpn.* **17**, 503 (1984).
11. Mims, C. A., and Krajewski, J. J., *J. Catal.* **102**, 140 (1986).
12. Vannice, M. A., *J. Catal.* **37**, 449 and 462 (1975).
13. Moore, S. E., and Lunsford, J. H., *J. Catal.* **77**, 297 (1982).
14. Kapteijn, F., Peer, O., and Moulijn, J. A., *Fuel* **65**, 1371 (1986).
15. Kapteijn, F., and Moulijn, J. A., "Final Report NOK-UGS," Project No. 4351-5, 1985.
16. Meijer, R., Weeda, M., Kapteijn, F., and Moulijn, J. A., *Carbon*, **29**, 929 (1991).
17. Kapteijn, F., Abbel, G., and Moulijn, J. A., in "Proceedings, Carbon '85, Kentucky," p. 181, 1985.
18. Cerfontain, M. B., Ph.D. thesis, University of Amsterdam, 1986.
19. Meijer, R., van der Linden, B., Kapteijn, F., and Moulijn, J. A., *Fuel*, **70**, 205 (1991).
20. Cerfontain, M. B., Meyer, R., Kapteijn, F., and Moulijn, J. A., *J. Catal.* **107**, 173 (1987).
21. Hermann, G., and Hüttinger, K. J., *Carbon* **24**, 705 (1986).
22. Hüttinger, K. J., *Carbon* **26**, 79 (1988).
23. Meijer, R., Mühlen, H.-J., Kapteijn, F., and Moulijn, J. A., *Fuel. Proc. Technol.* **28**, 5 (1991).
24. Mühlen, H.-J., and Sulimma, A., *Fuel. Proc. Technol.* **15**, 145 (1987).
25. Meijer, R., Ph.D. thesis, University of Amsterdam, 1991.